Ballistic chaotic quantum dots with interactions: A numerical study of the Robnik-Berry billiard

Ganpathy Murthy,[1] R. Shankar,[2] and Harsh Mathur[3]
[1]*Department of Physics and Astronomy, University of Kentucky, Lexington, Kentucky 40506-0055, USA*
[2]*Department of Physics, Yale University, New Haven, Connecticut 06520, USA*
[3]*Physics Department, Case Western Reserve University, Cleveland, Ohio 44106-7079, USA*
(Received 10 November 2004; revised manuscript received 8 June 2005; published 29 August 2005)

In previous work we have found a regime in ballistic quantum dots where interelectron interactions can be treated asymptotically exactly as the Thouless number g of the dot becomes very large. However, the results of the previous work depend on some assumptions concerning the renormalization group and various properties of the dot obeying random matrix theory predictions at scales of the order of Thouless energy. In the present work we test the validity of those assumptions by considering a particular ballistic dot, the Robnik-Berry billiard, numerically. While we find that many of our earlier predictions are borne out, some global aspects of our phase diagram need to be modified. With those modifications we conclude that, at least in the Robnik-Berry billiard, one can trust the results of our previous work at a qualitative and semiquantitative level.

DOI: 10.1103/PhysRevB.72.075364 PACS number(s): 73.50.Jt

I. INTRODUCTION

The quest for a satisfactory theory of quantum dots is driven not only by their obvious importance as mesoscopic devices revealed by a series of groundbreaking experiments,[1] but also by their challenge as a unique confluence of disorder, interactions, and finite-size effects.[2] For weak interactions, the universal Hamiltonian[3,4] (UH) provides a satisfactory description. For ballistic/chaotic quantum dots, we have espoused[5–7] an approach based on the fermionic renormalization group[8] (RG), $1/N$ expansions, and the fact that energy eigenstates around the Fermi energy in disordered systems ought to be described by random matrix theory (RMT).[9,10] Our approach not only explains the UH as a fixed point of the RG but also describes the physics outside its basin of attraction. It predicts a phase transition at strong coupling and allows a fairly detailed study[7] of the strong-coupling regime and the quantum critical region[11] separating it from that governed by the UH.

Our previous results,[5–7] however, were predicated on a variety of RMT and RG assumptions. To test our assumptions and the conclusions deduced from them, we have performed a detailed numerical study on a ballistic but chaotic billiard (the Robnik-Berry billiard[12]) and we report our findings here. It is important to note that our numerical work does not make any RG or RMT assumptions. Our results therefore provide an unbiased test of the assumptions underlying our previous work. While some of the assumptions we used are true only asymptotically at low energies, many of the physical predictions of our previous work are borne out. We also find that an important global feature of the previous phase diagram needs to be modified: We find, up to unavoidable mesoscopic fluctuations of our numerics, that the critical coupling in the large-g limit of the mesoscopic system (the same as the limit when the dot size becomes large) coincides with the bulk critical coupling, as has been suggested by Adam, Brouwer, and Sharma in a related problem.[13] In our previous work[7] we had concluded on the basis of an approximate cutoff scheme that the mesoscopic critical coupling was substantially less than the bulk one. However, all the qualitative properties of the various regimes were correctly described in our previous work.[7]

We recall the strategy and assumptions of our previous work[5–7] briefly so that the reader may see in advance what sort of ideas are put to test in our present study. In the primordial problem of interest to us, one has electrons confined to a ballistic dot of size L, with no impurities inside, and edges so irregular that classical motion is chaotic. The electrons experience the Coulomb interaction. In momentum space, all momenta within the bandwidth (of order k_F, the Fermi momentum) exist. The semiclassical ergodicization time for an electron within the dot is a few bounces, or $\tau_{\mathrm{erg}} \simeq L/v_F$. By the uncertainty principle this leads to an important energy scale, the Thouless energy $E_T \simeq \hbar v_F/L$, which has a dual significance. First, it controls the dimensionless conductance of a dot strongly coupled to leads, as follows. Since the transport through the dot takes place in a time such that energy is uncertain by an amount E_T, all single-particle states that fit into this band will each contribute a unit of dimensionless conductance. If the average single-particle level spacing is δ, then the dimensionless conductance is $g = E_T/\delta$. Second, in the other limit of dots very weakly coupled to leads (which we focus on in this work), the Thouless band (or Thouless shell) of width E_T centered on E_F, marks the scale within which RMT should apply to the energies and eigenfunctions[9] (more correctly, RMT should apply for eigenstates with energy separation $\Delta E \ll E_T$). In this context g is better denoted the Thouless number.

Note that the thermodynamic limit is a bit subtle in a ballistic dot. As $L \to \infty$, $E_T \to 0$ and the entire mesoscopic energy regime vanishes. In principle, one can imagine some mesoscopic physics occurring within this energy regime which is not smoothly connected to the bulk physics. Barring such a singular thermodynamic limit, it is to be expected that the large-g limit of the mesoscopic critical coupling should be identical to the bulk critical coupling.[13]

Since we are only interested in a narrow band of energies of width $E_T \ll E_F$ around E_F (the Thouless shell), the first step in the program[5] is to use the RG for fermions[8] to get an effective low energy theory by eliminating all momentum

states outside E_T. Should we worry that we are not eliminating exact single-particle eigenstates (labeled here by α)? No, because the disorder due to the boundaries will mix momentum states at roughly the same energy, and it does not matter whether we eliminate momentum states within any annulus of energy thickness E_T or the single-particle states they evolve into. Indeed, even the mixing within E_T is due to the fact that momentum itself is not well defined in a finite dot, a point we will elaborate on shortly. However, once we come down to within E_T of E_F, we cannot eliminate the remaining states in one shot since it is the flow of couplings *within* this band that is all important in the RG.

Now it is known[8] that the clean system RG (justified above) leads to Landau's Fermi-liquid interaction[14]

$$V = \sum_{\mathbf{k}\mathbf{k}'} F(\theta_{\mathbf{k}} - \theta_{\mathbf{k}'})\,\delta n(\mathbf{k})\,\delta n(\mathbf{k}'), \tag{1}$$

at an energy scale E_L which is small compared to E_F. But since E_L is a bulk scale it can always be made larger than E_T which vanishes as $L \to \infty$. Thus Murthy and Mathur[5] perform their RG on the Hamiltonian (focusing on the spinless case for simplicity),

$$H = \sum_{\alpha} c_{\alpha}^{\dagger} c_{\alpha} \varepsilon_{\alpha} + \sum_{\alpha\beta\gamma\delta} V_{\alpha\beta\gamma\delta} c_{\alpha}^{\dagger} c_{\beta}^{\dagger} c_{\gamma} c_{\delta}, \tag{2}$$

where

$$V_{\alpha\beta\gamma\delta} = \frac{1}{4} \sum_{\mathbf{k}\mathbf{k}'} F(\theta_{\mathbf{k}} - \theta_{\mathbf{k}'}) [\phi_{\alpha}^{*}(\mathbf{k}) \phi_{\beta}^{*}(\mathbf{k}') - \phi_{\beta}^{*}(\mathbf{k}) \phi_{\alpha}^{*}(\mathbf{k}')] \times [\phi_{\gamma}(\mathbf{k}') \phi_{\delta}(\mathbf{k}) - \phi_{\delta}(\mathbf{k}') \phi_{\gamma}(\mathbf{k})] \tag{3}$$

is simply the Landau interaction written in the basis of exact eigenstates, a statement that needs some elaboration. In usual RMT treatments, $\phi_{\alpha}(\mathbf{k})$ is the exact eigenstate α written in the infinite dimensional basis of all momentum states. In our version which uses the RG to reduce the Hilbert space, the states labeled by $\mathbf{k}$ are approximate momentum states with an uncertainty $\delta k \simeq 1/L$ in both directions. The number of such wave packets that fit into an annulus of radius k_F and thickness E_T/v_F is $\mathcal{O}(k_F L) = g$. We call them the wheel-of-fortune (WOF) states [see Fig. 1]. One way to construct such packets is to pick g plane waves of equally spaced momenta on the Fermi circle and to chop them off at the edges of the dot to respect the boundary conditions. This is what we mean by $\mathbf{k}$ in $\phi_{\alpha}(\mathbf{k}) = \langle \mathbf{k} | \alpha \rangle$.

We are now ready to state the two assumptions on which our previous work[5–7] was based. Assumption I: We assume that the g approximate momentum states generated as above form a complete basis for the g exact eigenstates in the Thouless shell. Assumption II: The energy eigenvalues ε_{α} obey RMT statistics as do the wave functions. For example, we assume that the ensemble averages (denoted by $\langle\rangle$) obey

$$\langle \phi_{\mu}^{*}(\mathbf{k}_1) \phi_{\mu}(\mathbf{k}_2) \phi_{\nu}^{*}(\mathbf{k}_3) \phi_{\nu}(\mathbf{k}_4) \rangle = \frac{\delta_{12}\delta_{34}}{g^2} + O(1/g^3) \tag{4}$$

Despite recent progress in ballistic billiards, this assumption remains to be proved.[15]

Assumption I seems remarkable—How can we furnish *in advance, independent of the dot shape* a basis of g states for expanding the g exact eigenstates within E_T? After all, these eigenstates are supposed to resemble those of a random matrix. The point is that no matter how chaotic the dot, it can only mix states at the same energy. While this sounds like Berry's ansatz,[16] it is somewhat different in both scope and content: Berry's ansatz states that every exact eigenstate α can be expanded in terms of an *infinite number* of $\mathbf{k}$ states (with the same energy $\epsilon_{\alpha} = \mathbf{k}^2/2m$) in the bulk, while we claimed[5–7] in our previous work that only g of WOF states are needed. Secondly, we claimed previously[5–7] that the *same* g WOF states can be used to describe all the states within the Thouless band.

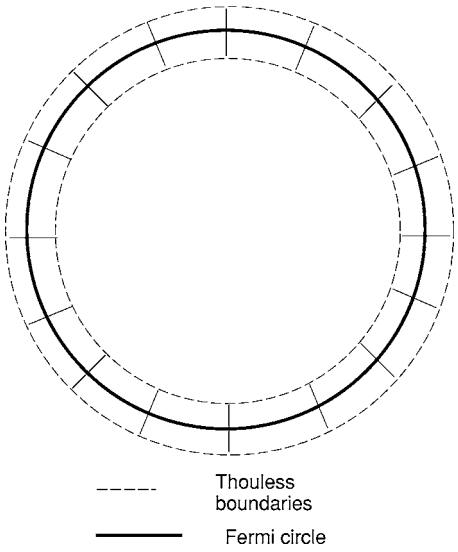

FIG. 1. The g wheel-of-fortune states in the Thouless band. They are packets in $\mathbf{k}$ space with average momenta equally spaced on the Fermi circle.

In this work, *without using RG assumptions or integrating states out*, we will show that Assumption I is true asymptotically deep in the Thouless shell, but becomes inaccurate as one moves to the edges of the Thouless shell. The WOF states are nearly orthonormal and the exact eigenstate right in the middle of the shell (that is, the state closest to E_F) has a 99.9% overlap with the WOF states. The success of this extension of Berry's conjecture to a finite dot exceeds our expectations in this regard. However, we find that the g WOF states become less effective at describing exact eigenstates as we move away from E_F towards the edges of the Thouless shell: The overlap drops to 50% at $E_{\alpha} = E_F \pm E_T/2$.

As for Assumption II, we have verified RMT behavior for the eigenvalues (as have others before us[17,18]) but not the eigenfunctions. Verifying Assumption II for the eigenfunctions requires more computational resources than we have, since one has to generate enough distinct dots to constitute an ensemble. What we did instead was to see to what extent the solution of a specific dot resembled the picture we drew based on these two assumptions. We find most of the expectations of our earlier work are borne out, but that the fluctuations in the effective potential are much larger than expected.

Given the fact that even if Assumption II were to be verified, Assumption I is valid only asymptotically deep in the

Thouless shell, and acquires increasing errors as one moves to the edges of the Thouless shell, how reliable are our earlier results?[5–7] In both the RG procedure and in the large-N mean approach, we used E_T as a cutoff in the RG sense. From this point of view, Assumption I represents a particular choice of cutoff function, which is inaccurate away from the center of the Thouless shell. It is well known from the RG literature[19] that while a different choice of cutoff can lead to differences in nonuniversal quantities, such as the critical temperature (or, in our case, critical coupling u^*), all universal properties such as the critical exponents or the behavior of correlators close to the critical point are independent of the choice of cutoff. In fact, in a model analogous to ours, but in which the correct dependence of the exact states on the analog of our WOF states could be exactly calculated, Adam, Brouwer, and Sharma[13] found that the critical coupling was $u^*=-2$ (for the spinless case). Using our incorrect cutoff function (based on Assumption I) would have resulted in $u^*=-1/\ln 2$, exactly as in our previous work.[5–7]

The correct value of the critical coupling is therefore likely to be $u^*=-2$ in our model as well.[13] Normally the value of the critical coupling is not a matter of serious concern, but here it coincides with the threshold of the bulk transition. So one might worry that the mesoscopic physics we outlined might get overturned by bulk physics for $|u|>|u|^*$. In a bulk Fermi-liquid theory in two dimensions, one expects a first-order transition at u^*, in which the order parameter (which is the Fermi surface distortion) jumps to a value of the order of E_L. More realistically, including terms normally neglected in Fermi-liquid theory,[20,21] one obtains a second-order transition in which the order parameter quickly reaches E_L. Given this, one must question our original strategy of using Shankar's RG to integrate out all states above the Thouless shell. As is intuitively clear, if a state is strongly affected by a phase transition in the low-energy subspace, then it should not be integrated out. If the bulk scenario also holds for the mesoscopic system, then the entire strong-coupling regime described in our previous work will be superceded by the bulk Pomeranchuk phase.[20,21]

We find that our numerical work confirms some of these expectations and clarifies the crossover between the weak- and strong-coupling phases. In work to be presented in the following sections, we assume that E_L is the entire bandwidth (Fermi-liquid theory is always valid). Note that we do not integrate out anything, nor do we use Shankar's RG. However, we find in our mesoscopic systems that the bulk transition is replaced by a smooth crossover. We do find that for $|u|>|u^*_{\rm bulk}|$ (and in some samples even for a substantial window of $|u|<|u^*_{\rm bulk}|$) that the order parameter exceeds the mesoscopic regime, but we never see any evidence for a first-order transition, as would be seen in a pure Fermi-liquid theory in the bulk.

We should note that there are subtleties in trying to observe a first-order transition in a finite system. If the order parameter is conserved, then a large jump in the order parameter can indeed be observed across the transition. However, in our case, the order parameter is not conserved and a bulk first-order transition must always be replaced by a crossover. Nevertheless, one can test for an incipient first-order transition by examining the structure of the static effective potential. If there are two minima in the effective potential with widely different values of the order parameter which cross in energy, then one infers a bulk first-order transition, whereas a single minimum (up to degeneracies forced by symmetry) which evolves continuously as a function of coupling indicates a second-order transition. Note that even in the first-order case, quantum fluctuations will allow tunneling between the minima in a finite system, which will convert the transition into a sharp crossover.

The bulk Fermi-liquid Pomeranchuk transition presents a pathological case where only a single minimum exists at any coupling (see the appendix for details). However, it is at zero order parameter for $|u|<|u^*|$ and at a large value of the order parameter $\approx E_F$ for $|u|>|u^*|$. Thus, though there is a single minimum, it changes discontinuously as a function of u.

We have examined the static mean-field effective potential for a number of disorder realizations, and we always find only a single minimum which evolves continuously with coupling. Thus, the bulk first-order transition has been modified into a second-order transition in our finite systems.

We can understand this partly as the effect of finite-size corrections on the clean bulk transition and partly as the effect of the chaotic scattering from the walls (see the appendix for details). However, somewhat surprisingly, we generically find a significant region of $|u|<|u^*_{\rm bulk}|$ for which the size of the order parameter is mesoscopic for the instability in an even Landau channel. This justifies our use of Shankar's RG in our previous work for $|u|<|u^*|$, but not for $|u|>|u^*_{\rm bulk}|$. However, we will argue that the physics of the strong-coupling regime, though not controlled by a mesoscopic energy scale, still possesses all the features that we identified in our earlier work.

We begin by describing how one starts from Eq. (3), which describes the effective Hamiltonian, and use our two assumptions with large-N ideas to make our predictions.[6,7] These predictions are expected to be asymptotically exact as $g\to\infty$.

First one expands the Landau function as

$$F(\theta)=\sum_m u_m e^{im\theta}. \tag{5}$$

Barring accidents, the phase transition occurs in one channel with some particular m (recall superconductivity). This allows us to focus on a single $u_m\neq 0$, ignoring all others. Then we carry out a Hubbard-Stratovich transformation on the interaction using a collective field $\boldsymbol{\sigma}$. We then formally integrate out the fermions and get an effective action $S(\boldsymbol{\sigma})$ for $\boldsymbol{\sigma}$. In this process we make use of Assumption II. The action in terms of $\boldsymbol{\sigma}$ is obtained by summing one loop Feynman diagrams with varying numbers of external $\boldsymbol{\sigma}$'s connected to a single fermion line running around the loop. Each diagram is a sum over fermion energy denominators multiplying products of a string of $\phi_\alpha(\mathbf{k})$'s. We are able to show that these products may be replaced by their ensemble averages in the large g limit. In other words the sum over so many terms in each diagrams leads to self-averaging. For the averages we use relations like Eq. (4). When this is done, the effective action can be cast into a form which has a g^2 in front of it,[6,7] so that the saddle point gives exact answers as $g\to\infty$.

At this point let us collect all the results and predictions of the RMT+large-N theory[7] with a view to comparing them with similar results without using Assumptions I and II on the Robnik-Berry billiard:

(i) In the large-g limit there is a sharp transition to a phase in which $\boldsymbol{\sigma}$ acquires a vacuum expectation value. The critical value of u_m in our approximation turns out to be $-1/\ln 2$ in the spinless case and $-1/2\ln 2$ in the spinful case. The true critical value is most likely to be the bulk value -2 (spinless) or -1 (spinful), as has been found in an explicitly solvable model by Adam, Brouwer, and Sharma.[13] This is an example of the nonuniversal quantity alluded to earlier, that we cannot predict exactly in our approach even as $g \to \infty$.

(ii) For finite g, instead of a sharp phase transition, there is a crossover from the weak-coupling regime through a quantum-critical regime to a strong-coupling regime. Due to the explicit symmetry breaking at order $1/g$, there is always some nonzero order parameter, which increases to a number of order g (in the normalization we use here, which is different from that of Ref.7) in the strong-coupling regime.

(iii) For symmetry breaking in odd angular momentum channels there are two exactly degenerate minima for every sample arising from time-reversal invariance.

(iv) The ground state energy at the minimum in the strong-coupling regime is lower than that in the weak-coupling regime by a number of order $g^2\delta$.

(v) The effective potential landscape in the strong-coupling regime is in the approximate shape of a Mexican hat, with the ripples at the bottom of the hat being of order $g\delta$.

(vi) In the quantum-critical and strong-coupling regimes, even low-energy quasiparticles acquire large widths given on average by

$$\Gamma(\varepsilon) \approx \frac{\delta}{\pi}\ln(\varepsilon/\delta). \tag{6}$$

We found that most of these predictions are verified by our numerical results on the Robnik-Berry billiard, except that the ripples at the bottom of the Mexican hat turn out to be much larger than expected for the $m=2$ Landau interaction channel.

II. THE ROBNIK-BERRY BILLIARD

In this section we will describe how the dot is chosen and how the single-particle energy levels ε_α and eigenfunctions $\phi_\alpha(\mathbf{r})$ are determined. We use a trick invented by Robnik and Berry[12] and elaborated upon by Stone and Bruus.[17] Consider a unit circle $|z|=1$ in the complex plane of $z=x+iy$. The analytic function

$$w(z) = \frac{z + bz^2 + cz^3 e^{i\chi}}{\sqrt{1+2b^2+3c^2}} \tag{7}$$

defines a map under which the unit circle in z gets mapped into a new shape in w, which will be our dot. The shape of the dot can be varied by varying the parameters b, c, and χ. The denominator ensures that the billiard has the same area (π) as the unit disc. The wave function $\phi_\alpha(w,\bar{w})=\phi_\alpha(u,v)$ is required to vanish at the boundary and obey

$$-\left(\frac{\partial^2}{\partial u^2}+\frac{\partial^2}{\partial v^2}\right)\phi_\alpha(u,v) = -4\frac{\partial}{\partial w}\frac{\partial}{\partial \bar{w}}\phi_\alpha(w,\bar{w}) = \varepsilon_\alpha\phi_\alpha(w,\bar{w}). \tag{8}$$

(We have chosen $\hbar=2m_b=1$, where m_b is the band mass.) If we now go the z plane where the wave function is $\phi_\alpha[w(z),\bar{w}(\bar{z})]$, the Schrödinger equation and boundary condition are

$$-4\frac{\partial}{\partial z}\frac{\partial}{\partial \bar{z}}\phi_\alpha(z,\bar{z}) = \varepsilon_\alpha |w'(z)|^2 \phi_\alpha(z,\bar{z}), \quad \phi_\alpha(|z=1|)=0, \tag{9}$$

where $w'(z)=dw/dz$. This differential equation in the continuum is next converted to a discrete matrix equation by writing

$$\phi_\alpha(z,\bar{z}) \equiv \phi_\alpha(r,\theta) = \sum_j \frac{1}{\gamma_j} C_j^\alpha \psi_j(r,\theta), \tag{10}$$

where $\psi_j(r,\theta)$ is the solution to the free Schrödinger equation in the unit disk vanishing on the boundary,

$$-\nabla^2\psi_j(r,\theta) = \gamma_j^2\psi_j(r,\theta). \tag{11}$$

(That is, these are Bessel functions in r times angular momentum eigenfunctions in θ.) Feeding this expansion into Eq. (9) one obtains the matrix equation

$$\sum_j M_{ij} C_j^\alpha = \frac{1}{\varepsilon_\alpha} C_i^\alpha, \tag{12}$$

where

$$M_{ij} = \frac{1}{\gamma_i}\langle i||w'|^2|j\rangle\frac{1}{\gamma_j}. \tag{13}$$

(Without the $1/\gamma_j$ in the expansion Eq. (10), M would not have been Hermitian.)

In practice one truncates M to a finite size, which in our case is 585 states. The computational limitation is not the diagonalization of the single-particle Hamiltonian, but the computation of the matrix elements of the interactions. One typically finds that the higher third of the states, not being subject to level repulsion due to the absence of even higher states, have very inaccurate energies.[17] We approximately corrected for this by fitting the calculated form of the energies to

$$\varepsilon_n = An\exp(Bn+Cn^3) \tag{14}$$

and then dividing the calculated energies by the exponential factor. This corresponds to an approximate "unfolding" transformation which keeps the density of states roughly constant.[17] Even this approach fails for the very highest 50 states, indicating that we cannot trust any result that involves the participation of these highest states.

The parameters of the conformal transformation b, c, and χ are chosen to lie in the range where classical behavior is chaotic, and where quantum chaos as reflected in the eigenvalue distribution has been established.[17] A value we used repeatedly was $b=c=0.2$, $\chi=0.85$. A nonzero χ ensures that

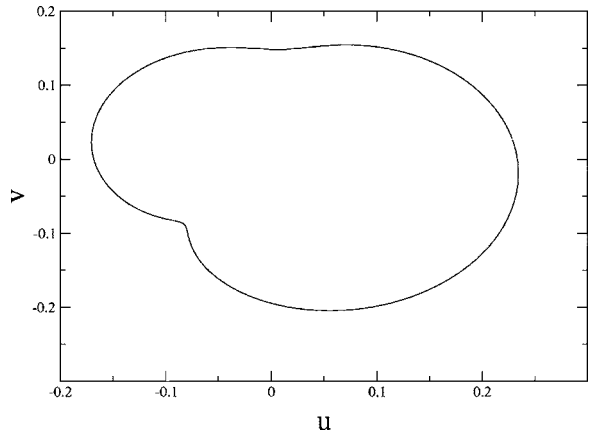

FIG. 2. The shape of the Robnik-Berry billiard for $b=c=0.2$, and $\chi=0.85$.

the billiard has no reflection symmetry. This shape is often called the Africa Billiard based on its resemblance to that continent, as seen in Fig. 2 for our chosen values of parameters.

We shall refer to these eigenfunctions and eigenvalues as exact even though they come from solving a truncated problem because we can easily increase the accuracy by increasing the size of the truncated Hilbert space.

A. Testing Assumptions I and II

Our ability to solve the Schrödinger equation (to high accuracy) implies in principle that we can test our two assumptions.

In the next section we will test Assumption I, i.e., see in detail how well the WOF states serve a basis within the Thouless band.

As for Assumption II, we and our predecessors[17,18] have shown that the eigenvalues and single eigenfunctions obey the distribution expected by RMT for a Gaussian Orthogonal Ensemble. [The ensemble is generated by varying the parameters in $w(z)$.]

Similar information about wave-function correlations is not known in the ballistic problem (despite some recent progress using supersymmetry methods[15]). We did not try to do this here since our computing capabilities did not allow us to generate an ensemble.

Instead we computed the fate of the interacting system without recourse to Assumptions I and II and compared this to our predictions based on these assumptions.

B. Completeness of the WOF basis

Let E_F be the Fermi energy. Then $g \simeq \sqrt{4\pi N} \simeq \sqrt{\pi E_F}$, which we arrive at as follows. The Fermi circle has a circumference $2\pi K_F$ and into this will fit $g=2\pi K_F/(2\pi/L)$ WOF states each of width $2\pi/L$ in the tangential direction. Finally $E_F=K_F^2/2m=K_F^2$, $N=k_F^2L^2/4\pi$ and $L=\sqrt{\text{Area}}=\sqrt{\pi}$.

As a test case when we picked the Fermi energy to be the 100th level, we found $g=37$. How well is this state $|F\rangle$ at E_F spanned by the g WOF states at the Fermi energy?

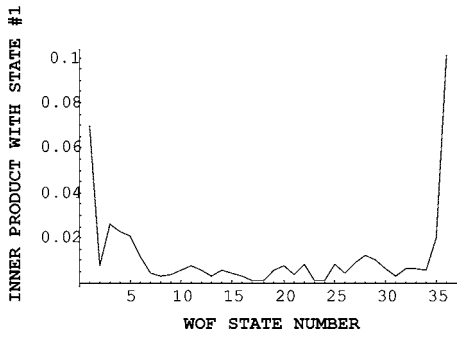

FIG. 3. The absolute value of $\langle n|1\rangle$, the inner product of WOF state number 1 with the other $g-1=36$ states.

First we first take g equally spaced points $\mathbf{k}_n$ on the Fermi circle and form the WOF states

$$\psi_{\text{WOF}-n}(\mathbf{r}) = \frac{1}{\sqrt{\pi}} e^{i\mathbf{k}\cdot\mathbf{r}} \Theta(\text{dot}) \tag{15}$$

where Θ(dot) is unity inside the dot and zero outside. These states are very close to being orthonormal. For example, the overlaps of $n=1$ state (with $\mathbf{k}$ along the y axis) with the others as we go around the circle is shown in Fig. 3.

Next we ask how much of the state $|F\rangle$ at the Fermi energy is contained in the WOF states. We find $\Sigma_{n=1}^{g}|\langle n-\text{WOF}|F\rangle|^2=0.9993$. This is a rather remarkable result. It says that $|F\rangle$, which is a vector with 585 components (which was the size of our truncated problem) can be expanded almost completely in terms of $g=37$ WOF states which are given in advance. In other words, as one changes the shape of the dot and works at fixed Fermi energy, the state $|F\rangle$ changes in a random way, but that randomness is only in which particular combination of WOF states describes it, not in the completeness of the WOF basis.

While this is very satisfactory we need more to implement our scheme: we need to expand all g states in the WOF basis. Here we find that as we move off the center of the Thouless band, the fractional norm captured by the WOF basis drops. In a typical case, with $g=37$, there are roughly 12 states (one-third of g) where the number lies above 95%. At band edge, this drops to 50%, as shown in Fig. 4. Thus there is inevitably some error in transcribing the Landau interaction written in terms of the WOF states labeled by $\mathbf{k}$ into the basis of g exact eigenstates labelled by α. This just means that the location of the critical point will not be correctly predicted by our RMT-based analysis, as pointed out recently by Adam, Brouwer, and Sharma.[13]

This concludes our (partial) test of Assumptions I and II. We turn to a comparison of our results based on these assumptions with a direct solution of the problem with no recourse to the assumptions.

C. Hartree-Fock solution of the interacting problem

How can the knowledge of the "exact" eigenfunctions and eigenvalues in the billiard help in the solution of the problem with interactions? The tactic will be illustrated in schematic form first. Suppose we have a four-Fermi interaction added

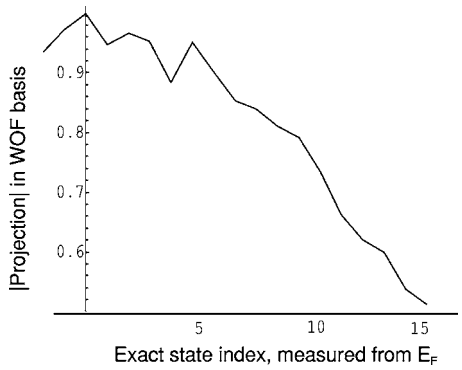

FIG. 4. The norm of the projection of the nth exact eigenstate from E_F on to the subspace spanned by the WOF states. It can be seen that more and more of the exact eigenstate lies outside this subspace as one moves away from E_F.

to a free Hamiltonian which in first quantization is given by some differential operator H_0. Then the path integral becomes

$$Z = \int d\psi d\bar{\psi} e^S, \tag{16}$$

where

$$S = \int d\tau \left[\bar{\psi}(i\partial_\tau - H_0)\psi + \frac{u}{2}(\bar{\psi}\psi)^2 \right]. \tag{17}$$

Using a Hubbard-Stratanovich transformation we can write

$$Z = \int d\psi d\bar{\psi} d\sigma e^S, \tag{18}$$

where

$$S = \int d\tau \left[\bar{\psi}[i\partial_\tau - H_0 + \sigma]\psi - \frac{\sigma^2}{2u} \right]. \tag{19}$$

If the fermions are integrated out we will get an effective action $S_{\text{eff}}(\sigma)$. *To find the minimum we need just the action for static* σ. In this case it is clear that

$$\int d\psi d\bar{\psi} \exp\left[\int d\tau \bar{\psi}[i\partial_\tau - H_0 + \sigma]\psi \right] = e^{-E_0(\sigma)T}, \tag{20}$$

where $T \to \infty$ is the length of the imaginary time τ axis and $E_0(\sigma)$ is the ground state energy of $\psi^\dagger(H_0+\sigma)\psi$. To find $E_0(\sigma)$ one simply solves for the single-particle levels of $(H_0+\sigma)$ and fills up the ones with negative energy. The effective action for static configurations, which is also the effective potential, is

$$V_{\text{eff}} = E_0(\sigma) + \frac{\sigma^2}{2u}. \tag{21}$$

At this point we have a mean-field theory. We still need to justify its use by showing that fluctuations of the collective field $\boldsymbol{\sigma}$ around its minimum are small. In our previous work, based on Assumptions I and II we showed that the fluctuations were indeed small in the limit of large g, since the g^2 in front of the actions limits fluctuations. In the billiard we justify the mean field similarly, based on the large depth and curvature of the minimum.

When the Landau interaction is factorized, the Hamiltonian whose ground state gives us $E_0(\sigma)$ is

$$\sum_{\alpha\beta} \psi_\alpha^\dagger(\delta_{\alpha\beta}\varepsilon_\beta - \boldsymbol{\sigma}\cdot\mathbf{M}_{\alpha\beta})\psi_\beta, \tag{22}$$

where, for the case $m=1$, for example,

$$\mathbf{M}_{\alpha\beta} = \sum_{\mathbf{k}} \phi_\alpha^*(\mathbf{k})\phi_\beta(\mathbf{k})\frac{\mathbf{k}}{k}, \tag{23}$$

and α, β, and $\mathbf{k}$ are not restricted to the Thouless band. This is because we want to solve the problem without any of the assumptions that led to the effective low-energy theory within the Thouless band. Note that $\boldsymbol{\sigma}$ has two components, because the Landau interaction associated with u_m has two parts,

$$V_L = \frac{u_m}{2}\sum_{\mathbf{k}\mathbf{k}'} \delta n_{\mathbf{k}}\delta n_{\mathbf{k}'}(\cos m\theta_{\mathbf{k}} \cos m\theta_{\mathbf{k}'} + \sin m\theta_{\mathbf{k}} \sin m\theta_{\mathbf{k}'}). \tag{24}$$

Once S_{eff} is known (on a grid of points in the $\boldsymbol{\sigma}$ plane), one can ask if and when the minimum moves off the origin.

So far our considerations have been fairly generic, and the Landau interaction has been written in momentum space. However, in testing our approach in the billiard, we will find it more convenient to represent the Landau interaction in real space, since the eigenfunctions are known as linear combinations of Bessel functions whose integrals are best carried out in real space. We have carried out calculations for two Laudau parameters corresponding to $m=1$ and $m=2$. The $m=1$ Landau interaction is chosen to be (in second-quantized notation)

$$\frac{1}{2}\int d^2r \Psi^\dagger(\vec{r})\frac{1}{(2m_bH_0)^{1/4}}(-i\vec{\nabla})\frac{1}{(2m_bH_0)^{1/4}}\Psi(\vec{r}) \cdot \times \int d^2r' \Psi^\dagger(\vec{r}')\frac{1}{(2m_bH_0)^{1/4}}(-i\vec{\nabla}')\frac{1}{(2m_bH_0)^{1/4}}\Psi(\vec{r}'), \tag{25}$$

where for clarity we have temporarily restored the explicit dependence on the band mass m_b. The factors of $1/(2m_bH_0)^{1/4}$ on each side of the ∇ have the effect of $1/|\mathbf{k}|$ in momentum space. Since momentum does not commute with the free Hamiltonian H_0, the factors have to be placed symmetrically. Note that this corresponds only to the $\vec{q}=0$ part of the Landau interaction. In reality, all values of $\vec{q}$ up to the scale E_L/v_F exist in the Hamiltonian. Depending on the shape of the dot a particular combination of them may break symmetry to give the best energy. Still, we expect that since at large g we are close to the zero-dimensional limit, the best combination will consist largely of very small $\vec{q}$ parts of the Landau interaction. In any case, the energy of the true symmetry-broken state can only be lower than what we calculate, so what we have here is a conservative estimate of symmetry breaking. Similarly the $m=2$ interaction (also at $\vec{q}=0$) is

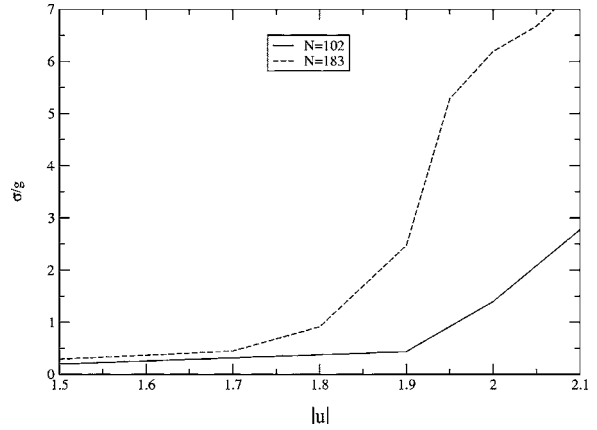

FIG. 5. The absolute value of the order parameter normalized by g as a function of coupling strength u for two values of the number of particles N for $m=2$. The order parameter does indeed scale approximately like g but there are evidently large mesoscopic fluctuations. Note that nothing discontinuous happens at the bulk critical coupling strength $|u^*_{\text{bulk}}|=2$.

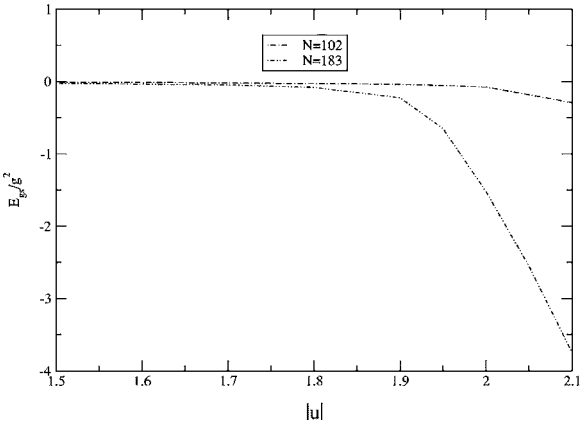

FIG. 6. Reduction in ground state energy normalized by g^2 for two values of the number of particles N for $m=2$.

$$\frac{1}{2}\int d^2r\Psi^\dagger(\vec{r})\frac{1}{(2m_bH_0)^{1/2}}(\nabla_x^2-\nabla_y^2)\frac{1}{(2m_bH_0)^{1/2}}\Psi(\vec{r})\cdot$$
$$\times\int d^2r'\Psi^\dagger(\vec{r}')\frac{1}{(2m_bH_0)^{1/2}}[(\nabla')_x^2-(\nabla')_y^2]\frac{1}{(2m_bH_0)^{1/2}}\Psi(\vec{r}')$$
$$+\frac{1}{2}\int d^2r\Psi^\dagger(\vec{r})\frac{1}{(2m_bH_0)^{1/2}}2\nabla_x\nabla_y\frac{1}{(2m_bH_0)^{1/2}}\Psi(\vec{r})$$
$$\times\int d^2r'\Psi^\dagger(\vec{r}')\frac{1}{(2m_bH_0)^{1/2}}2(\nabla')_x(\nabla')_y\frac{1}{(2m_bH_0)^{1/2}}\Psi(\vec{r}'). \tag{26}$$

The integrals are over $(w,\bar{w})$, but can be converted to integrals over the disk by using the conformal mapping of Eq. (7). Of course, the derivative operators must also be transformed in the process. In order to find the matrix elements of $\mathbf{M}_{\alpha\beta}$ we had to take the matrix elements of the above operators in the basis of exact billiard states. We carried out the angular part of the integrals analytically, but had to turn to numerical integration to evaluate the radial integrals. This is a computationally intensive calculation, but once the matrix $\mathbf{M}$ has been constructed, one simply diagonalizes the Hamiltonian of Eq. (22) for a mesh of $\boldsymbol{\sigma}$ in the plane, adds up the energies of the lowest N particles to obtain the fermionic ground state energy, and obtains the effective potential landscape from Eq. (21) for various values of the coupling strength u. After this, it is a simple matter to identify the global minimum, which gives us the lowering of ground state energy and the value of the order parameter as a function of u.

Let us proceed to the results, displayed in pictorial form. In Fig. 5 we show the absolute value of the order parameter, normalized by the nominal value of $g=\sqrt{4\pi N}$, for two values of the number of particles N. The bulk transition happens at $|u^*_{\text{bulk}}|=2$. As can be seen, there is a nonzero order parameter for any nonzero $|u|>1.5$, and it grows smoothly and continuously as u increases. Nothing discontinuous happens at $|u|=2$ or even beyond, indicating that the instability does not suddenly become first order at the bulk value of u^*. As explained in the introduction, we always see only a single continuously evolving minimum in the mean-field effective potential up to a double degeneracy forced by time-reversal symmetry in the $m=1$ case. Of course, in these finite systems, the Thouless and bulk scales are related by a factor $g/4\pi$, which is not that large. So somewhere between $u=1.9$ and $u=2.1$ the instability seems to reach the bulk scale. However, note that the size of systems we have considered correspond quite closely to actual ballistic samples,[1] which typically have a few hundred electrons. Further, the expectation value of $|\boldsymbol{\sigma}|$ is consistent our earlier estimate[7] (based on RMT assumptions) that it should be order g. However, there are large mesoscopic fluctuations as one approaches the bulk critical point.

In Fig. 6 we show the corresponding reduction in ground state energy normalized by g^2. Once again, the curves track each other fairly closely for $|u|<2$, indicating that the energy reduction due to interactions is indeed of order g^2, as predicted by our earlier analytical estimates.[7]

In Fig. 7 we show the effective potential landscape for $m=2$, with $N=102$, at a value of $u=2$, at which the minimum is well developed, but the order parameter is still of the order of the nominal Thouless scale and has not reached the bulk scale. The RMT analysis predicted a Mexican hat landscape with "small" ripples (down by $1/g$) in the circle of minima of the Mexican hat. The landscape we see bears no resemblance to this. Instead, it appears to be an isolated minimum at a nonzero $\boldsymbol{\sigma}$. Upon close inspection it can be seen that the minimum is shallower in the transverse direction than in the radial direction, but this is the only indication we could find of a (perhaps) incipient Mexican hat structure.

Figure 8 shows a similar effective potential landscape for symmetry breaking in the $m=1$, channel for $N=102$, and $u=2.08$, where the two exactly degenerate minima expected from time-reversal invariance considerations can be seen. The landscape also appears more Mexican-hat-like than in the $m=2$ case.

To trace the origin of this difference in behavior, we investigated the average absolute value $\langle|M^i_{\alpha\beta}|\rangle$ and the rms

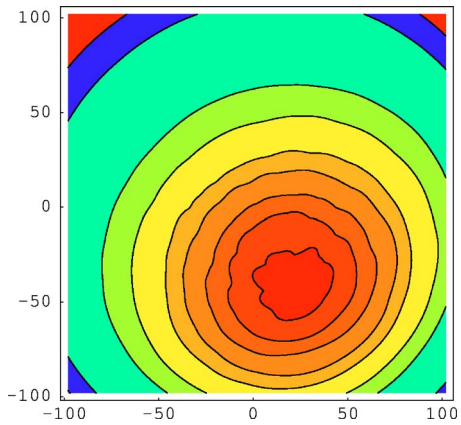

FIG. 7. (Color online) Effective potential landscape for symmetry breaking in the $m=2$ channel at $N=102$, $u=2.00$. Instead of a Mexican hat minimum structure with small ripples we see an isolated minimum. The minimum does seem shallower in the transverse direction.

deviation of the matrix elements from the mean absolute value, $\sqrt{\langle|M^i_{\alpha\beta}|^2\rangle-\langle|M^i_{\alpha\beta}|\rangle^2}$ for the two cases $m=1,2$. The results for the $i=1$ (corresponding to ∇_x for $m=1$ and $\nabla_x^2-\nabla_y^2$ for $m=2$) shown in Fig. 9 are an energy average for a particular billiard, with the parameters $b=c=0.20$, $\delta=0.85$. (We have confirmed similar behavior of the matrix elements for other parameter values as well.) Figure 9 shows these quantities as a function of the energy difference between the two states α and β. There are two features that are particularly noteworthy: (i) There is a "hole" in the $m=1$ matrix element near zero energy difference, and (ii) the rms deviation of the $m=2$ matrix elements from their mean absolute value is huge. As a rough estimate, if the matrix elements were Gaussian distributed complex numbers, the rms deviation should be roughly half the mean modulus.

However, the $i=2$ component (corresponding to ∇_y for $m=1$ and $2\nabla_x\nabla_y$ for $m=2$) shows very different behavior in Fig. 10. While the $m=1$ case looks similar to the $i=1$ component, the fluctuations of the $m=2$, $i=2$ component are strongly suppressed by almost an order of magnitude below the mean.

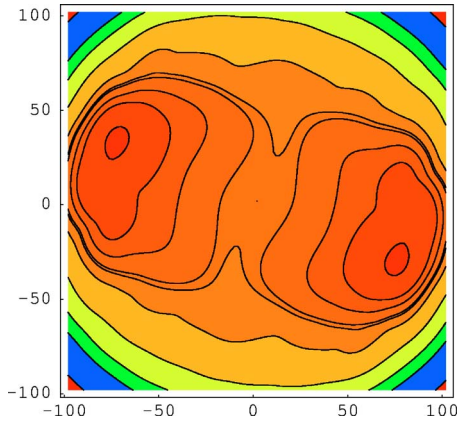

FIG. 8. (Color online) Effective potential landscape for symmetry breaking in the $m=1$ channel for $N=102$ and $u=2.08$. The two exactly degenerate minima required by time-reversal invariance can be seen, as can a Mexican-hat-like structure.

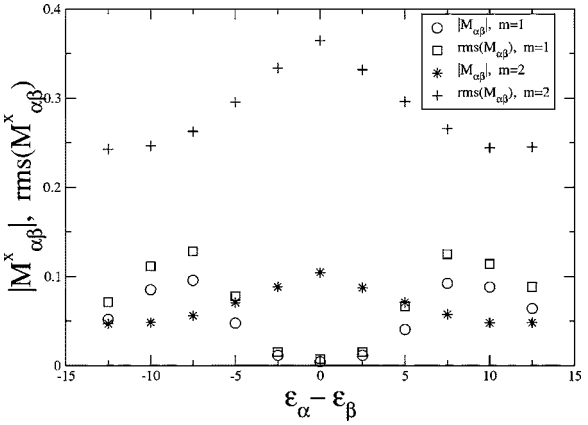

FIG. 9. A plot of the absolute value and the rms deviation of the matrix elements $M^x_{\alpha\beta}$ from their mean absolute value as a function of $\varepsilon_\alpha-\varepsilon_\beta$ for the two cases $m=1,2$.

Consider first the "hole" at E_F for $m=1$. By symmetry considerations alone, one can understand that the diagonal matrix element $M_{\alpha\alpha}$ for $m=1$ has to be zero, sample by sample, in the absence of an external magnetic field. Focusing on the x component of the order parameter,

$$M^x_{\alpha\alpha}=\sum_{\mathbf{k}}\cos(\theta_{\mathbf{k}})\phi^*_\alpha(\mathbf{k})\phi_\alpha(\mathbf{k}). \tag{27}$$

By time-reversal invariance $\phi^*_\alpha(\mathbf{k})=\phi_\alpha(-\mathbf{k})$. Noting that $\theta_{-\mathbf{k}}=\theta_{\mathbf{k}}+\pi$, and that the cos term changes sign, one concludes that $M_{\alpha\alpha}=-M_{\alpha\alpha}=0$. The reason the "hole" persists for finite energy differences for the operator $\vec{p}=-i\vec{\nabla}$ can be explained by noting that[22] for a billiard,

$$\vec{p}=im[\vec{r},H]$$

$$\Rightarrow(-i\vec{\nabla})_{\alpha\beta}=-im(\vec{r})_{\alpha\beta}(\varepsilon_\alpha-\varepsilon_\beta), \tag{28}$$

which means that the matrix element must vanish at least linearly with the energy difference. In fact, such "banded" matrix elements have been found for many operators in ballistic dots.[23]

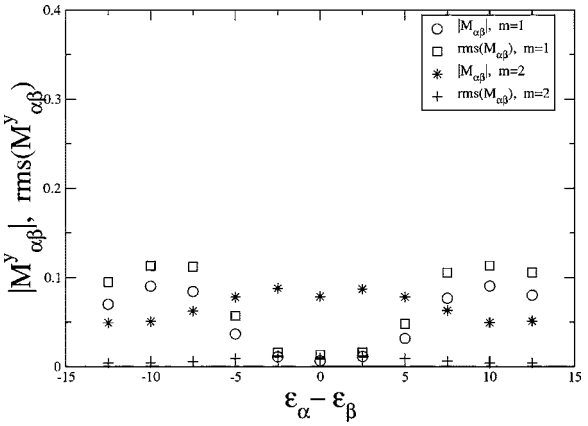

FIG. 10. A plot of the absolute value and the rms deviation of the matrix elements $M^y_{\alpha\beta}$ from their mean absolute value as a function of $\varepsilon_\alpha-\varepsilon_\beta$ for the two cases $m=1,2$.

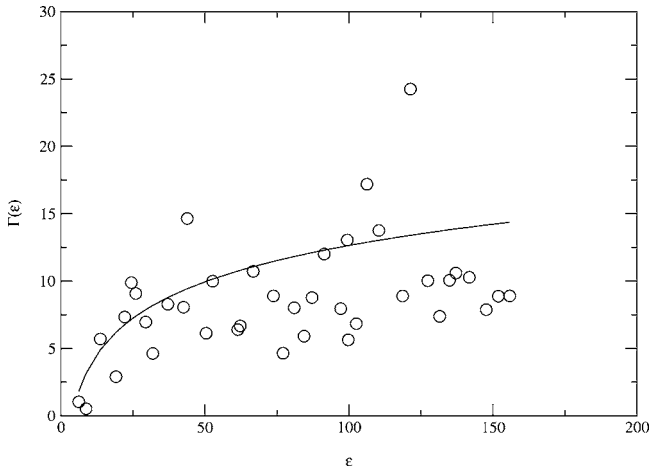

FIG. 11. A plot of the decay width of quasiparticles induced by their coupling to fluctuations of the collective field $\boldsymbol{\sigma}$, for $N=183$, $m=2$, and $u=1.8$. The solid line is the theoretical prediction for the quantum critical regime from our previous RMT-based analysis (Ref. 7). While the prediction does well on average, there are huge variations in the widths due to large variations in how strongly each level couples to the collective mode.

Consider next the fact that the distribution of the matrix elements of $M^x_{\alpha\beta}$ for the $m=2$ case is much broader than for the $m=1$ case, while the $M^y_{\alpha\beta}$ matrix elements have a very narrow distribution. The RMT answer would have the rms deviation of $M_{\alpha\beta}$ from the mean to be of the same order as the mean absolute value. This seems to be roughly true for both components of $m=1$ but grossly untrue for the $i=1$ component of $m=2$. Since it is these mesoscopic fluctuations in $M_{\alpha\alpha}$ which determine the size of the ripples at the bottom of the Mexican hat in the RMT scenario, this broad distribution of $M_{\alpha\beta}$ seems to be the cause of the failure of the RMT prediction that the ripples should be subdominant by $1/g$. While it is tempting to try to explain this in relation to the shape of the billiard (Fig. 2), which certainly appears to favor an x^2-y^2 type of symmetry, a satisfactory explanation of the broad distribution of the $m=2$, $i=1$ matrix elements eludes us.

Our knowledge of the eigenfunctions at the global minimum allow us to compute the effective action for time-dependent $\boldsymbol{\sigma}$ at that minimum. Since the quasiparticles couple to this collective field, the interaction induces a decay width for the quasiparticles (details can be found in Ref. 7). In Fig. 11 we compare the numerically calculated values of the width to the parameter-free theoretical prediction (solid line) in the quantum-critical regime based on RMT.[7] The RMT-based prediction seems consistent with the numerics, though there is a lot of variation in the widths driven by large variations in the matrix elements coupling the quasiparticle levels to the collective mode. In this particular sample, note that the coupling is *weaker* than the critical coupling. This provides an example of a sample which exhibits robust symmetry breaking even in the nominal weak-coupling regime due to mesoscopic fluctuations.

III. CONCLUSIONS

In our earlier work, we used a global RG assumption[8] to reduce the problem on the scale of the Thouless energy to that of a disordered noninteracting problem with Fermi-liquid interactions. This is quite plausible for ballistic dots on very general grounds, as long as the Fermi surface remains circular. To proceed further we had to make two further assumptions: (i) that the g approximate momentum states at the Fermi energy were a good basis in which to expand the exact disorder eigenstates, and (ii) that the wave functions of the exact eigenstates in the momentum basis obeyed all the statistical properties of RMT. Based on these two assumptions we were able to construct a solution to the problem[5–7] which was asymptotically exact in the limit $g\to\infty$. This solution led to specific predictions for various physical quantities, including the size of the order parameter, the reduction in energy due to interactions, the shape of the energy landscape, and the size of the quasiparticle decay widths.

Soon after our original work, it was pointed out by Adam, Brouwer, and Sharma[13] that the correct value of the critical coupling is probably the bulk value $u^*=-2$ for the spinless model in the $g\to\infty$ limit (as compared to our[5,6] value of $-1/\ln 2$). As pointed out in the introduction, this error is the result of taking Assumption I to be true throughout the Thouless shell, whereas it is true only asymptotically deep within it. Adam, Brouwer, and Sharma also noted that the bulk transition of pure Fermi liquid is first order in two dimensions, and has an order parameter (Fermi surface distortion) of the order of $E_L\approx E_F$, one might worry that the mesoscopic physics of the strong-coupling regime ($|u|>|u^*|$) uncovered by us[6,7] would be superceded by bulk physics. Also, if and when this does occur, our use of Shankar's RG to integrate states above E_T would be incorrect for $|u|>|u^*|$. We have argued that this first-order transition is not generic and requires fine tuning to a strictly constant density of states and a pure Fermi-liquid form for the interactions. Any deviation from this fine tuning, such as a varying density of states due to finite-size effects, or interactions beyond the Fermi-liquid form, are dangerously irrelevant,[19] and lead to a generic second-order transition.[20,21]

In this paper we explicitly eschewed the RMT and RG assumptions that we made in previous work with a view to independently testing their validity. Thus, the fact that our present numerical results are consistent with our previous analytical estimates (as detailed below) argues strongly for the qualitative correctness of the assumptions we used in our earlier work.[5–7] Note that our calculation is still predicated on the validity of the Fermi-liquid form of the interactions on a scale E_L much larger than the Thouless energy E_T. In retaining this assumption we are on firm ground, since after all, the Thouless energy can be made as small as one wishes merely by increasing the size of the system. We also assumed that the mean-field description of the Landau Fermi-liquid interactions is valid, which is justified by the fact that the minima in the effective potential landscape are indeed of order $g^2\delta$.

We found that our Assumption I, that the approximate momentum states were a good basis in which to expand the exact disorder eigenstates, was extremely good near the Fermi energy, but became increasingly inaccurate as one went to the edge of the Thouless shell. We did not test Assumption II about wave-function correlations explicitly, but indirectly through its effects on the predictions of our earlier work.

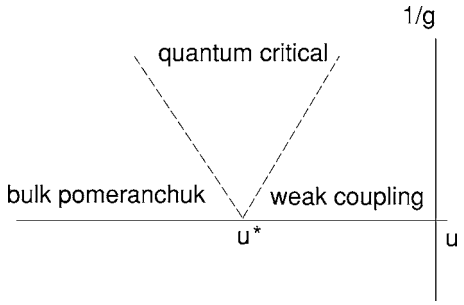

FIG. 12. The phase diagram of a quantum dot undergoing a Pomeranchuk instability. The critical point is the same as that for bulk Fermi-liquid theory, which is recovered in the $g \to \infty$ limit. The region to the right of the critical point is the weak-coupling regime, with the origin being described by the universal Hamiltonian. The region marked quantum critical represents a regime dominated by collective quantum Fermi surface fluctuations. The region to the left of the critical point is the bulk Pomeranchuk regime, and the order parameter is expected to be of the order of the bulk scale E_L there.

We found a smooth crossover near $u \approx u^*$, with no indication of a first-order bulk-type transition. As explained in the introduction, one needs to examine the static effective potential in order to distinguish the order of the transition. We always find a single minimum in our mean-field effective potential which evolves continuously with the coupling, indicating that the crossover does not have a first-order character in our finite systems. We believe this smoothing of the first-order bulk transition is the result of a combination of finite-size corrections to the density of states and the effects of chaotic scattering at the walls (see the appendix for details). Generically, *any* deviation from pure bulk Fermi-liquid theory is expected to destabilize the first-order transition. We do find that the Fermi surface distortion no longer lies in the mesoscopic regime for $|u| > |u^*|$. This thus leads us to modify the physical picture of the strong-coupling regime. In our earlier work, we believed it to be a regime controlled by the mesoscopic energy scale E_T, but we find that in fact it is controlled by the bulk energy scale E_L. Since we expect the Laudau interactions to be substantially modified in this regime by the Fermi surface distortion, we can no longer quantitatively trust our earlier predictions. However, since the crossover between these scales is smooth, we believe that the qualitative features that we identified in the strong-coupling regime, namely, an order parameter and broad quasiparticles, will continue to be valid in the bulk regime as well. Our current understanding of the phase diagram is summarized in Fig. 12.

An important feature of the numerics, which we had not anticipated in our earlier work, is that in a substantial window $|u| < |u^*|$ the order parameter is mesoscopic in certain samples, and that there are huge mesoscopic fluctuations in the order parameter for $|u| < |u^*|$. This means that even systems ostensibly in the weak-coupling regime can display a substantial symmetry-breaking due to a combination of mesoscopic fluctuations and interaction effects. Our results are expected to be of relevance to realistic ballistic quantum dots, since these have roughly a hundred electrons,[1] similar to our billiard. It would be desirable to have greater statistics on these mesoscopic fluctuations, which we leave for future work.

We also found that as long as the order parameter was mesoscopic, most of the predictions of our earlier work were consistent with the numerics, with the exception of the shape of the effective potential landscape in the case of symmetry-breaking in the $m=2$ channel. Even here, the minimum is shaped more like a crescent, indicating the possible emergence of the Mexican hat structure at larger values of g (we went to the largest value of g that we could given that we kept only 585 states and had to keep at least half the states empty). We traced the discrepancy back to the anomalously broad distribution (compared to estimates based on a complex Gaussian distribution) of the matrix elements $M^x_{\alpha\beta}$. However, we were unable to pin down a physical reason for this broad distribution for the $m=2$ case.

In conclusion, much of the physics we uncovered using our RMT assumptions seems to be valid in the Robnik-Berry billiard. The second-order transition that we uncovered in the $g \to \infty$ limit seems to indeed be broadened into a smooth croossover as expected, belying fears that it may be overtaken by a first-order bulk transition. The strong-coupling regime, which we believed to be a mesoscopic regime in our earlier work, is now seen to be a regime controlled by bulk physics. Perhaps the most interesting feature from the point of view of experiments is that mesoscopic fluctuations are strong enough for there to be a substantial symmetry breaking for systems quite far from the bulk critical coupling. However, even when the order parameter is mesoscopic, RMT does not seem to completely describe the mesoscopic fluctuations of the effective potential. The question of how large g has to be before RMT becomes fully applicable remains open; another way to phrase the question is to ask what the nonuniversal corrections to RMT are in ballistic systems. Finally, an important open question is whether the broad distributions of matrix elements of interaction operators is a generic feature of ballistic systems, rather than being a special feature of the Robnik-Berry billiard, and if so, what physics determines the width of those distributions. However, our results here give us encouragement that the RG and RMT assumptions made in our previous work can indeed be used with confidence in making predictions in ballistic systems, at a qualitative and semiquantitative level so long as the Fermi surface distortion remains mesoscopic.

ACKNOWLEDGMENTS

We would like to thank Yoram Alhassid, Alex Barnett, Piet Brouwer, and Doug Stone for illuminating conversations, and the Aspen Center for Physics where part of this work was carried out. We are also grateful to the NSF for partial support under Grants Nos. DMR 0311761(G.M.) and DMR 0354517(R.S.).

APPENDIX

In this appendix we will show that the first-order Pomeranchuk instability of the bulk two-dimensional (2D) Fermi liquid is the result of a very special fine tuning of parameters.

The inclusion of finite-size effects in the clean Fermi-liquid theory will be shown to make the Pomeranchuk instability second order.

Let us consider the theory in the 2D bulk first. The Hamiltonian for the $q=0$ sector is

$$\mathcal{H} = \sum_{\mathbf{k}} [\varepsilon(\mathbf{k}) - \varepsilon_F]\delta n(\mathbf{k}) + \frac{1}{2\rho(\varepsilon_F)} \sum_{\mathbf{k},\mathbf{k}'} f(\mathbf{k},\mathbf{k}')\delta n(\mathbf{k})\delta n(\mathbf{k}'). \tag{29}$$

Here

$$\rho(\varepsilon_F) = \left. \frac{dN(\varepsilon)}{d\varepsilon} \right|_{\varepsilon_F} \tag{30}$$

is the density of states at the Fermi energy. Let us consider a single channel of the Landau interaction for which $f(\mathbf{k},\mathbf{k}') = u_m \cos m(\theta\text{-}\theta')$. The original Fermi surface is circular. We consider a Fermi surface distortion with amplitude σ in the m^{th} Landau channel,

$$\delta n(\mathbf{k}) = \mathrm{sgn}(\cos m\theta); \quad \varepsilon(\mathbf{k}) \leqslant \sigma \cos m\theta, \tag{31}$$

and zero otherwise, where $\mathrm{sgn}(x)$ denotes the sign of x. The kinetic energy is readily converted into an energy integral,

$$KE = \int \frac{d\theta}{2\pi} \int_0^{\sigma \cos m\theta} \rho(\varepsilon)(\varepsilon - \varepsilon_F) d\varepsilon. \tag{32}$$

Assuming a constant density of states, which is true for the two-dimensional bulk, the integration can be carried out to give

$$KE = \rho(\varepsilon_F)\frac{\sigma^2}{4}. \tag{33}$$

Turning now to the interaction energy, we decompose the Landau interaction as in Eq. (24) to see that only the $\cos m\theta \cos m\theta'$ term matters, and obtain

$$PE = \frac{u_m}{2\rho(\varepsilon_F)} \left[\int \frac{d\theta}{2\pi} \cos m\theta \int_0^{\sigma \cos m\theta} d\varepsilon \rho(\varepsilon) \right]^2, \tag{34}$$

which leads, under the same assumption of a constant density of states, to

$$PE = \rho(\varepsilon_F)\frac{u\sigma^2}{8}. \tag{35}$$

Thus the total energy for a Fermi surface distortion of amplitude σ is

$$E(\sigma) = \rho(\varepsilon_F)\frac{\sigma^2(2+u)}{8} \tag{36}$$

The instability is at $u^* = -2$. This is the exact energy of a Fermi surface distortion in bulk 2D Fermi-liquid theory. Note the striking feature that there are no higher powers of σ, which would be generically expected in a Landau-Ginzburg type expansion of the free energy in the order parameter. This is due to the special nature of the Fermi-liquid interaction, and the fact that the density of states is constant. Another aspect of this very special nature of the bulk instability can be seen in the fact that the Pomeranchuk susceptibility diverges as $1/(2+u)$ as in any second-order transition, but the order parameter itself has a discontinuity at the transition. This shows that the first-order transition (in the order parameter) is a fine-tuned version of a second-order transition, and is not robust against perturbations. Such perturbations, which are formally irrelevant in the RG sense, but which must not be neglected at the critical point, are known as *dangerous irrelevant* operators in the critical phenomenal literature.[19] A more general bulk theory along the lines of Refs. 20,21 would include such dangerous irrelevant interactions neglected by Fermi-liquid theory, and a renormalization of the kinetic energy, which effectively means that the density of states is not constant. Such treatments lead to a generic second-order transition.

However, our model has only the Fermi-liquid interaction, albeit in a finite system with closed boundary conditions. It is known that in a finite two-dimensional system, the number of states below ε is given by the generalized Weyl asymptotic formula[24]

$$N(\varepsilon) = \frac{Am\varepsilon}{4\pi} - \frac{\mathcal{L}\sqrt{m\varepsilon}}{4\pi} + \cdots, \tag{37}$$

where the higher order terms are subleading. Here A is the area of the system, m is the effective mass of the particle, and $\mathcal{L}$ is the perimeter of the system. This leads to the density of states near the Fermi energy

$$\rho(\varepsilon) = \frac{Am}{4\pi}\left[1 - \frac{\mathcal{L}}{2A\sqrt{m\varepsilon_F}} + \frac{\mathcal{L}}{4A\sqrt{m\varepsilon_F}}\frac{\delta\varepsilon}{\varepsilon_F} - \frac{3\mathcal{L}}{16A\sqrt{m\varepsilon_F}}\frac{\delta\varepsilon^2}{\varepsilon_F^2} + \cdots \right]. \tag{38}$$

It is now a straightforward exercise to compute the energy of the Fermi surface distortion of Eq. (31). It is

$$E(\sigma) = \rho(\varepsilon_F)\left[\frac{\sigma^2(2+u)}{8} - \frac{\mathcal{L}}{512A\sqrt{m\varepsilon_F}}\frac{\sigma^4(9+6u)}{\varepsilon_F^2} + \cdots \right]. \tag{39}$$

Near the instability, $u \approx -2$, the σ^4 term is seen to be small but positive. This means that finite-size effects have made the transition truly second order in both senses: the susceptibility diverges at the transition and the order parameter varies continuously through the transition.

Let us restate this important result: The appearance of a first-order transition in the 2D bulk system (as far as the order parameter is concerned) is a result of special fine tuning, and does not survive generic renormalizations or finite-size corrections, which make the transition second order, even in the absence of quantum chaos.

Realizing that $A\sqrt{m\varepsilon_F}/\mathcal{L} \approx k_F\mathcal{L} \approx g$ and $\varepsilon_F \approx g^2\delta$, we can write the additional term as

$$\frac{\sigma^4}{g^5}. \tag{40}$$

The above is for a clean system. The introduction of chaotic boundary scattering, insofar as it can be modeled by RMT as

in our earlier work,[7] also produces such a term, but with a much larger magnitude for large g,

$$\frac{\sigma^4}{g^2}. \tag{41}$$

We must keep in mind that this is true only if the Fermi surface distortion is mesoscopic.[7] It is clear that the effects of quantum chaos dominate the effects of finite size corrections, and render the growth of the order parameter slower when it is mesoscopic. Putting both the finite-size and the effect of chaotic scattering together, we can infer that near u^* the order parameter will increase as g as long as it is mesoscopic, crossing over to increasing as $g^{5/2}$ for large Fermi surface distortions. If bulk terms beyond Fermi-liquid theory are added, the order parameter will increase as g^2 far beyond the mesoscopic scale.

[1] U. Sivan, R. Berkovits, Y. Aloni, O. Prus, A. Auerbach, and G. Ben-Yoseph, Phys. Rev. Lett. **77**, 1123 (1996); S. R. Patel, S. M. Cronenwett, D. R. Stewart, A G. Huibers, C. M. Marcus, C. I. Duruoz, J. S. Harris, K. Campman, and A. C. Gossard, Phys. Rev. Lett. **80**, 4522 (1998); F. Simmel, D. Abush-Magder, D. A. Wharam, M A. Kastner, and J P Kotthaus, Phys. Rev. B **59**, R10441 (1999); D. Abusch-Magder *et al.*, Physica E (Amsterdam) **6**, 382 (2000); F. Simmel, T. Heinzel, and D. A. Wharam, Europhys. Lett. **38**, 123 (1997); J. A. Folk, S. R. Patel, K. M. Bimbaum, C. M. Marcus, C. I. Duruoz, and J. S. Harris, Phys. Rev. Lett. **86**, 2102 (2001); S. Lüscher T. Heinzel, K. Ensslin, W. Wegscheider, and M. Bichler, Phys. Rev. Lett. **86**, 2118 (2001).

[2] For recent reviews, see, T. Guhr, A. Müller-Groeling, and H. A. Weidenmüller, Phys. Rep. **299**, 189 (1998); Y. Alhassid, Rev. Mod. Phys. **72**, 895 (2000); A. D. Mirlin, Phys. Rep. **326**, 259 (2000).

[3] A. V. Andreev and A. Kamenev, Phys. Rev. Lett. **81**, 3199 (1998); P. W. Brouwer, Y. Oreg, and B. I. Halperin, Phys. Rev. B **60**, R13977 (1999); H. U. Baranger, D. Ullmo, and L. I. Glazman, Phys. Rev. B **61**, R2425 (2000); I. L. Kurland, I. L. Aleiner, and B. L. Al'tshuler, Phys. Rev. B **62**, 14886 (2000).

[4] I. L. Aleiner, P. W. Brouwer, and L. I. Glazman, Phys. Rep. **358**, 309 (2002), and references therein; Y. Oreg, P. Brouwer, X. Waintal, and B. Halperin, *Nano-Physics and Bio-Electronics*, (Elsevier, New York, in press), and references therein.

[5] G. Murthy and H. Mathur, Phys. Rev. Lett. **89**, 126804 (2002).

[6] G. Murthy and R. Shankar, Phys. Rev. Lett. **90**, 066801 (2003).

[7] G. Murthy, R. Shankar, D. Herman, and H. Mathur, Phys. Rev. B **69**, 075321 (2004).

[8] R. Shankar, Physica A **177**, 530 (1991); R. Shankar, Rev. Mod. Phys. **66**, 129 (1994).

[9] K. B. Efetov, Adv. Phys. **32**, 53 (1983); B. L. Al'tshuler and B. I. Shklovskii, Sov. Phys. JETP **64**, 127 (1986).

[10] M. L. Mehta, *Random Matrices* (Academic Press, San Diego, 1991).

[11] S. Chakravarty, B. I. Halperin, and D. R. Nelson, Phys. Rev. Lett. **60**, 1057 (1988); Phys. Rev. B **39**, 2344 (1989); For a detailed treatment of the generality of the phenomenon, see, S. Sachdev, *Quantum Phase Transitions* (Cambridge University Press, Cambridge, 1999).

[12] M. Robnik, J. Phys. A **17**, 1049 (1984); M. V. Berry and M. Robnik, J. Phys. A **19**, 649 (1986).

[13] S. Adam, P. W. Brouwer, and P. Sharma, Phys. Rev. B **68**, 241311(R) (2003).

[14] A. A. Abrikosov, L. P. Gorkov, and I. E. Dzyaloshinski, *Methods of Quantum Field Theory in Statistical Physics* (Dover Publications, New York, 1963).

[15] K. B. Efetov and V. R. Kogan, Phys. Rev. B **67**, 245312 (2003).

[16] M. V. Berry, J. Phys. A **10**, 2083 (1977).

[17] A. D. Stone and H. Bruus, Physica B **189**, 43 (1993); Surf. Sci. **305**, 490 (1994).

[18] Y. Alhassid and C. H. Lewenkopf, Phys. Rev. B **55**, 7749 (1997), and references therein.

[19] K. G. Wilson, Rev. Mod. Phys. **47**, 773 (1975).

[20] C. Varma, Phys. Rev. Lett. **83**, 3538 (1999), cond-mat/0311145 (2003).

[21] V. Oganesyan, S. A. Kivelson, and E. Fradkin, Phys. Rev. B **64**, 195109 (2001).

[22] A. H. Barnett (private communication, 2004).

[23] A. H. Barnett, "Asymptotic rate of quantum ergodicity in chaotic Euclidean billiards", Courant Institute preprint, 2004.

[24] H. P. Bates and E. R. Hilf, *Spectra of Finite Systems* (Mannheim: BI Wissenschaftsverlag, 1978).